Electric fields on quasiperiodic potentials

2010 J. Phys.: Condens. Matter 22 115501

(http://iopscience.iop.org/0953-8984/22/11/115501)

IOP Publishing Journal of Physics: Condensed Matter

J. Phys.: Condens. Matter **22** (2010) 115501 (9pp) doi:10.1088/0953-8984/22/11/115501

Electric fields on quasiperiodic potentials

F Salazar and G Naumis

Departamento de Física-Química, Instituto de Física, Universidad Nacional Autónoma de México (UNAM), Apartado Postal 20-364, 01000, México, Distrito Federal, Mexico

Received 14 November 2009, in final form 3 February 2010
Published 5 March 2010
Online at stacks.iop.org/JPhysCM/22/115501

Abstract

The effects of an electric field on the electronic spectrum and localization properties of quasiperiodic chains are studied. As quasiperiodic systems, we use the Harper and the Fibonacci potentials since we prove that both are closely interrelated. In the limit of a strong field, a ladder spectrum with localized states is observed. The ladder structure can be understood by using perturbation theory. Then each local isomorphism class of the quasiperiodic potential reproduces its structure in the ladder. In the case of a weak field, we observed that the singular spectrum of the quasiperiodic potential tends to be smoothed, and the gaps decrease linearly with the field. Such an effect can be understood using a variational approach, perturbation theory and a series of approximants. When the electric field and the quasiperiodic potential have the same order of magnitude, it is possible to observe a delocalization effect due to local resonances.

(Some figures in this article are in colour only in the electronic version)

1. Introduction

After the first quasicrystalline alloy was discovered in 1984 [1], quasiperiodic potentials have been studied intensively. Such kinds of alloys present a structure which is neither periodic nor disordered, with diffraction patterns that present Bragg peaks with non-crystallographic symmetries [2]. In order to understand the quasicrystal properties such as transport, localization or diffusion, different one-dimensional quasiperiodic potentials have been studied, particularly the Harper model and the Fibonacci chain [3–7]. For the Fibonacci chain, the spectrum is singularly continuous [2, 8]. The corresponding eigenfunctions are critical, and show self-similarity and multifractality [2, 9]. In some sense, real quasicrystals are disappointing because they do not exhibit such kinds of exotic features. Instead their transport properties are similar to those observed in amorphous semiconductors [10]. Although there is a lot of work concerning the nature of conductivity in quasiperiodic potentials [11, 12], it is surprising that the problem of explaining why there is a disagreement between experimental and theoretical work has not received much attention. In a series of previous works, we showed that the spectrum of quasiperiodic systems is very unstable against disorder [13–18]. In fact, the transport properties for two and three dimensions for quasiperiodic potentials have not been completely understood [19–21].

A second source of disagreement is a problem that, although it has been explored by some groups [22–24], its importance for conductivity has not been thoroughly recognized by the scientific community. In the presence of an external uniform electric field (F), the energy spectrum changes. For periodic potentials and when interband transitions are not considered, the electron wavefunctions have time-periodic oscillations called Bloch oscillations. In the case of the single-orbital tight-binding model, the electric field can localize all eigenstates [25], and the energy spectrum is a ladder of discrete and equally spaced levels known as a Wannier–Stark ladder (WSL) [26, 27]. If phonons are not considered, the band is tilted and, due to Bragg reflection at the band edges, the electron is confined with a localization length given by $l_B = B/eF$, where B is the bandwidth and e is the electron charge. There are two regimes of interest as a function of the localization length and electric field: (i) material effects dominate when $l < l_B$ and (ii) the electric field dominates when $l > l_B$. For non-periodic potentials under strong fields, described by the single-orbital tight-binding model, all eigenstates are factorially localized and their spectra are Stark ladders with non-uniform spacing [25]. The structure of the ladder for the Harper and Fibonacci potentials has been studied by Niizeki *et al* [28]. They concluded that the structure of the Fibonacci ladder presents many discontinuities while the Harper ladder presents a periodic behavior when the phase of the quasiperiodic potential is changed (corresponding to different local isomorphism classes). Under weak electric fields, there are several numerical studies which present a paramount fact: the fractal spectrum of a quasiperiodic

system tends to be smoothed since the spectral gaps tend to disappear, changing the spatial behavior of the electronic wavefunction [23, 24, 29]. This behavior has been studied numerically, although there is no clear explanation for this fact. In this paper, we present a complete study of the behavior of the Fibonacci and Harper potentials under an electric field in the limits of strong and weak fields. To achieve such a goal, we use perturbation theory and periodic approximants of the quasiperiodic potentials. Furthermore, using a previous result by our group [30], we can understand in a simple way the differences in the Fibonacci and Harper ladders that were obtained by Niizeki *et al* [28]

It is worthwhile mentioning that semiconductor superlattices have been used to study WSL experimentally, since the electric field needed to observe these phenomena are easily accessible due to the large effective lattice spacing. In particular, for GaAs–AlAs superlattices, an effective blueshift of the optical absorption edge accompanied by an electron-optical oscillation of the absorption coefficient has been observed [31, 32]. Recently, an optical analog of the electronic Bloch oscillations has been reported with light transport through periodic dielectric systems [33].

The layout of this paper is the following, in section 2 we present the models, in sections 3 and 4 we study the cases of strong and weak electric fields. In section 5 we study the localization properties when the field is applied, and finally the conclusions are given in section 6.

2. The model

We start by setting the main features of the model. Here we will consider a chain with lattice parameter $a = 1$ and periodic boundary conditions. The Hamiltonian in the Wannier representation has the form

$$H_C = \sum_j V(j)|j\rangle\langle j| - \sum_j (t|j\rangle\langle j+1| + t|j+1\rangle\langle j|), \quad (1)$$

where t is the hopping between nearest-neighbor atoms j and $j+1$, and $V(j)$ is the self-energy for the site j. When a uniform electric field (F) is applied in the parallel direction to the system, there is an extra term in the potential:

$$H_F = F\sum_j |j\rangle j\langle j|. \quad (2)$$

The complete Hamiltonian is written as

$$H = H_C + H_F. \quad (3)$$

Through the paper, two choices for H_C are used: the Harper and Fibonacci potentials. The Harper potential was derived to describe one electron on a two-dimensional square lattice under a perpendicular uniform magnetic field. The Harper potential in the Wannier representation is [30]

$$V(j) = 2\lambda\cos(2\pi\omega j + \varphi)|j\rangle\langle j|, \quad (4)$$

where $|j\rangle$ is the Wannier state localized on site j and φ is a phase factor that produces different isomorphisms of the lattice. For rational ω, this potential can be solved using Bloch's theorem [34]. For irrational ω, the spectrum depends on the localization–delocalization parameter λ. All eigenstates are extended and the energy spectrum is continuous when $\lambda < 1$. If $\lambda > 1$, all eigenstates are localized and the spectrum is made from pure points, while for $\lambda = 1$, the wavefunctions are critical and the spectrum is singular continuous.

The Fibonacci chain is one of the most studied quasiperiodic systems in one dimension. In the on-site problem (diagonal model), the diagonal elements $V(j)$ of the Hamiltonian take two values: ϵ_A or ϵ_B following a Fibonacci sequence. This sequence can be built considering two letters A and B, and the substitution rules, $A \to AB$ and $B \to A$. If one defines the first generation sequence as $\mathcal{F}_1 = A$, the subsequent chains are generated using the substitution rules. For instance, $\mathcal{F}_2 = AB$, $\mathcal{F}_3 = ABA$ and $\mathcal{F}_4 = ABAAB$. Each generation is labeled with an index l, and the number of letters in each generation l is given by the Fibonacci numbers $F(l)$, which can be obtained from the relation $F(l) = F(l-1) + F(1-2)$, with the initial conditions $F(0) = 1$, $F(1) = 1$. In [30], we proved that a generalized potential which contains the Fibonacci sequence can be written as

$$V(j) = \langle V\rangle + \delta V(\{j\omega + \varphi\} - \{(j+1)\omega + \varphi\}), \quad (5)$$

where $\{x\}$ is the decimal part function, $\delta V = \epsilon_A - \epsilon_B$ and $\langle V\rangle = \epsilon_A\omega + \epsilon_B(1-\omega)$. It is worth mentioning how ω determines the kind of sequence. For rational ω, the sequence is periodic while for irrational ω the sequence is quasiperiodic. In fact, for ω equal to the golden mean $\tau = (\sqrt{5}-1)/2$, a Fibonacci potential is obtained. For the rational approximants of τ, the formula produces a sequence of approximant crystals. For example, when $\omega = 1$ the sequence potential is $\epsilon_A\epsilon_A\epsilon_A\epsilon_A\cdots$, which corresponds to the linear chain, when $\omega = 1/2$ the sequence is $\epsilon_A\epsilon_B\epsilon_A\epsilon_B\epsilon_A\epsilon_B\cdots$, which corresponds to a diatomic chain, and so on. With the aid of equation (5), it is possible to study the Fibonacci approximants and understand the electron behavior in the transition from a periodic to a quasiperiodic potential.

Now let us compare the effects of applying an electric field to a periodic and a quasiperiodic system. To do this, we diagonalized the Hamiltonian given by equation (1) for a periodic and a Fibonacci chain with 1300 sites using periodic boundary conditions. Figure 1(a) shows the energy spectrum for a periodic chain with self-energy $\epsilon = 1$ and hopping $t = 1$. The open black circles correspond to $F = 0$ and the open gray circles to $F = 1$. Notice how the bandwidth changes drastically as well as the overall shape of the spectrum. The inset figure 1(a′) shows an amplification of the spectrum for $F = 0$ (black open circles). Two states for each energy level are clearly observed as a consequence of the periodic boundary conditions (double degeneration). However, there are two energy levels without degeneration localized in the edge of the bandwidth. When $F = 1$, the energy levels are equally spaced and the electric field breaks the degeneration as shown in figure 1(a″) (gray open circles). Such a kind of spectrum is called a Stark ladder [26].

In figure 1(b), the case of the Fibonacci on-site chain is presented with $\epsilon_A = 1$, $\epsilon_B = 0$ and $t = 1$. The open black

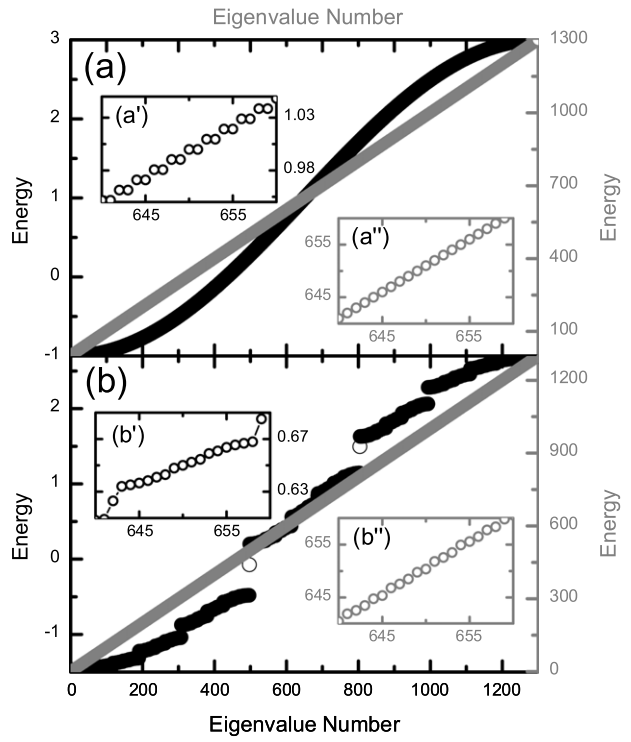

Figure 1. Energy spectrum for a chain with 1300 sites. In (a) linear chain with $F = 0$ (black circles) and $F = 1$ (gray circles). In the inset we show an amplification for $F = 0$ (a′) (open black circles) and for $F = 1$ (a″) (open gray circles). In (b) a Fibonacci chain with $F = 0$ (black circles) and $F = 1$ (gray circles). In the insets (b′) and (b″) we present an amplification of the spectrum.

circles correspond to $F = 0$. As is well known, a fractal set of minibands is obtained. Figure 1(b′) shows the energy levels with non-equal spacing (open black circles). The gray line corresponds to $F = 1$. Notice how the gaps tend to be closed. Furthermore, the spectrum is similar to the ladder obtained in the periodic case.

In conclusion, figure 1 presents the two limits that we are going to consider. In the case of a strong field, determined by the criterion $l > l_B$, H_F is dominant and the quasiperiodic potential H_C is basically a perturbation to the solution of the pure electric case. The other limit, $l < l_B$, is the case of a weak field, where H_C is dominant and the electric field term H_F is basically a perturbation. In the following two sections, we show in detail how perturbation theory allows us to understand the effects of the field in these two limits.

3. Strong electric field

In this section we will consider the case of a strong field, i.e. $l > l_B$. For this limit, the non-perturbed Hamiltonian is H_F. The jth eigenvalue of H_F is $E_j^{(0)} = Fj$, and the eigenfunctions are localized on site j, i.e. the amplitude of the eigenfunction j at site l is given by $\psi_j(l) = \delta(j - l)$. With these conditions in mind, we will explore in general the effects of adding a perturbing potential $V(j)$ such that $H_C = V(j)$. According to the time-independent perturbation theory, the energy correction to $E_j^{(0)}$ is given by [35]

$$E_j^{(1)} \approx \langle \Psi_j | H_C | \Psi_j \rangle, \tag{6}$$

where $|\Psi_j\rangle$ is an eigenstate of H_F such that $H_F|\Psi_j\rangle = E_j^{(0)}|\Psi_j\rangle$. However, $|\Psi_j\rangle = \sum_{l=1}^{N} \psi_j(l)|l\rangle$, from where it follows that

$$E_j^{(1)} \approx \sum_{l,l',n} \psi_j^*(l)\psi_j(l)V(n)\langle l'|n\rangle\langle n|l\rangle$$
$$= \sum_l |\psi_j(l)|^2 V(j) = V(j),$$

where we used that the wavefunction is localized. This general result is valid for any potential and indicates that the correction to the eigenvalue j is the potential evaluated precisely at the site j. Now we look to the particular case of a quasiperiodic potential. In the case of Harper, the energy levels are given by

$$E(\varphi) \equiv E_j^{(0)} + V(j) = Fj + 2\lambda\cos(2\pi\omega j + \varphi). \tag{7}$$

Such a simple result explains the dispersion relation between E versus φ (that we will denote as $E(\varphi)$) that was reported some time ago by Niizeki *et al* [28] from numerical simulations. In [28], periodic oscillations were observed in the energy levels as a function of the phase (φ). The oscillations are just given by the second term in equation (7). According to Niizeki *et al* [28], the situation is quite different for a Fibonacci potential, since a discontinuous dispersion relation is observed. Using the perturbation approach developed here, we can understand the difference between the Harper and Fibonacci potentials as follows. Let us consider equation (5). The decimal part function has period 1, and it can be developed as a Fourier series [30]:

$$\{x\omega + \varphi\} = \frac{1}{2} - \frac{1}{\pi}\sum_{s=1}^{\infty}\frac{1}{s}\sin[2\pi s(x\omega + \varphi)]. \tag{8}$$

By using equation (8) in (5)

$$V(j) = \langle V\rangle + \delta V\left(-\frac{1}{\pi}\sum_{s=1}^{\infty}\frac{1}{s}\sin[2\pi s((j+1)\omega + \varphi)]\right.$$
$$\left. + \frac{1}{\pi}\sum_{s=1}^{\infty}\frac{1}{s}\sin[2\pi s(j\omega + \varphi)]\right),$$

and the identity $\sin A - \sin B = 2\cos[\frac{1}{2}(A+B)]\sin[\frac{1}{2}(A-B)]$ the potential is written as

$$V(j) = \langle V\rangle + \delta V\left(\frac{2}{\pi}\sum_{s=1}^{\infty}\tilde{V}(s)\cos[\pi s((2j+1)\omega + 2\varphi)]\right) \tag{9}$$

where

$$\tilde{V}(s) \equiv \frac{\sin(\pi s\omega)}{\pi s}. \tag{10}$$

$\tilde{V}(s)$ will be referred to as the sth Fibonacci harmonic. Notice that each term of the series contains a $\cos[\pi s((2j+1)\omega + 2\varphi)]$ which corresponds to a Harper potential. Thus the Fibonacci potential can be obtained as a sum of Harper potentials. Each Harper potential has a weight given by the Fibonacci harmonics [30]. We can follow the change from a Harper to a

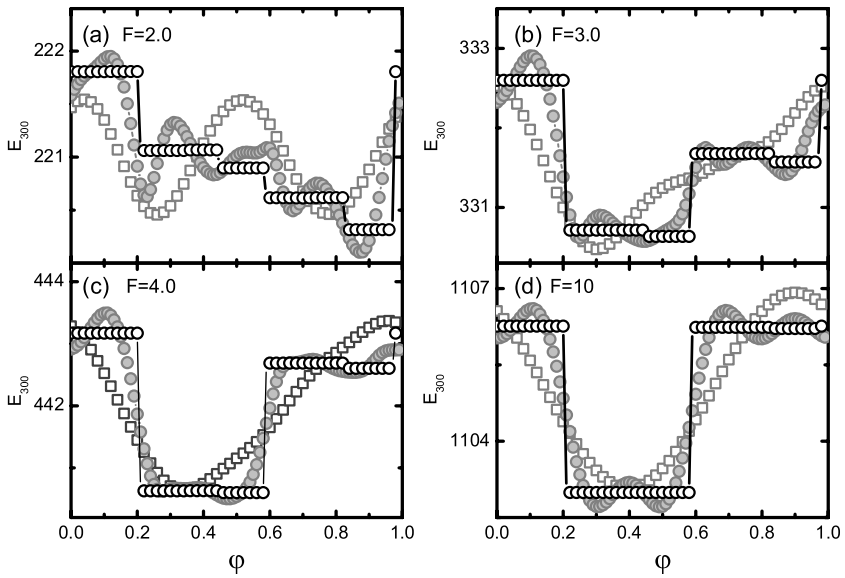

Figure 2. Dispersion relation $E(\varphi)$ for the eigenvalue 300 in a chain with 377 sites and different electric fields (a) $F = 2.0$, (b) $F = 3.0$, (c) $F = 4.0$ and (d) $F = 10$. The Fibonacci potential (open circles) is obtained as a sum of Harper potentials with a weight given by the Fibonacci harmonics. The first (open squares) and fourth (gray circles) Fibonacci harmonics show the transition process. When a strong electric field is applied, the dispersion relation is a square well that corresponds to the Fibonacci potential (d).

Fibonacci spectrum just by adding harmonics, since the energy levels in the presence of the electric field are given by

$$E(\varphi) = Fj + \langle V\rangle + \delta V\left(\frac{2}{\pi}\sum_{s=1}^{\infty}\frac{1}{s}\sin(\pi s\omega) \times \cos[\pi s((2j+1)\omega + 2\varphi)]\right). \quad (11)$$

Such a result can be confirmed by obtaining the spectrum by a direct diagonalization of the Hamiltonian given by equation (1), and using equation (9) to fill $V(j)$. Figure 2 shows the evolution of the dispersion relation $E_j(\varphi)$ for the eigenvalue 300 (E_{300}) using different electric fields. All chains have 377 sites, and the parameters used in this figure are $\omega = (\sqrt{5}-1)/2$, $\epsilon_A = 1-\omega$, $\epsilon_B = -\omega$ and $\lambda = 1$. The transition from the Harper to the Fibonacci dispersion relation is presented in figures 2(a)–(d) for different electric fields. The pure Harper potential, corresponding to the first Fibonacci harmonic, is shown in figure 2 with open squares. The fourth is shown with gray circles, while the full Fibonacci potential corresponds to open circles. The panels correspond to the fields (a) $F = 2.0$, (b) $F = 3.0$, (c) $F = 4.0$ and (d) $F = 10$. Notice how the increase of harmonics makes the dispersion relation closer to the Fibonacci chain (open circles). In particular, figure 2 shows how the dispersion relation takes the form of a square wavefunction, which is exactly the shape of the Fibonacci potential, while the harmonics are just the first terms of the series that approximate the square wavefunction. Such a result is in perfect agreement with the theoretical prediction.

4. Weak electric field

In this section, we consider the limiting case of a quasiperiodic chain with a weak field such that $l < l_B$ ($F/\lambda \ll 1$). As shown in figure 1, the weak electric field has a tendency to close the energy gaps. To understand the problem, we study the transition process from $F = 0$ to some given field $F \neq 0$. Figure 3 shows the energy levels for a chain with 1300 sites for different Fibonacci approximants (a) $\omega = 1/2$, (b) $\omega = 3/5$ and (c) $\omega = 8/13$. All gaps can be appreciated when $F = 0$ (open black circles) for all of the three cases. In order to see the transition process, we show the eigenvalues for different electric fields, as shown in the figure. One can see the closing of the energy gaps with an increasing field. In order to determinate how the gaps disappear as a function of the electric field, we define

$$\Delta E_g(F) \equiv (E_n(F) - E_{n-1}(F))/(E_n^0 - E_{n-1}^0), \quad (12)$$

where $E_n(F) - E_{n-1}(F)$ is the difference between two energy eigenvalues at the edges of a gap for some F and $E_n^0 - E_{n-1}^0$ is the same energy eigenvalue difference for $F = 0$. The ratio ΔE_g is presented in the inset of each figure. In figure 3(a′), only one gap is present and its size decreases linearly with the field. In figures 3(b′) and (c′), the first gaps labeled with the letter A are presented by black circles. The second gap, labeled with B, is plotted with open black circles. The secondary gaps C and D are also plotted with open gray circles and open gray squares, respectively. Notice that in all cases the path follows a linear behavior. The ratio for the gaps in the approximant $\omega = 8/13$ also follows a linear behavior too.

Now we will use perturbation theory to understand why the gaps are reduced in this regime. For weak fields, we can consider H_C as the unperturbed Hamiltonian and H_F as a perturbation. We present how this transition is achieved for the first rational approximants. The energy spectrum for a monatomic chain ($V(j) = \epsilon$) with N atoms and periodic boundary conditions is

$$E^{(0)}(k) = \epsilon + 2t\cos k, \quad (13)$$

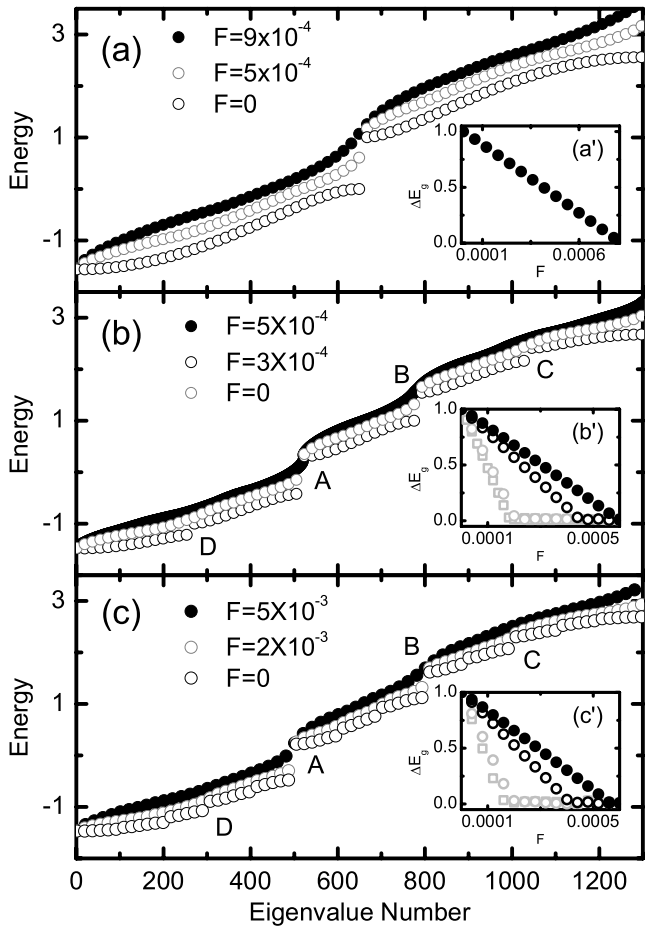

Figure 3. Energy levels for different Fibonacci approximants (a) $\omega = 1/2$, (b) $\omega = 3/5$ and (c) $\omega = 8/13$. In each figure, three different electric fields are shown. The first one corresponds to $F = 0$ (open black circles), where all gaps can be appreciated, another one corresponds to one electric field that closes all energy gaps (black circles) and the last one (open gray circles) is a field that shows the transition process, where its magnitude is indicated in each figure. In (b) and (c), the gaps are labeled with the letters A, B (main gaps), C and D (minor gaps). The ratio $\Delta E_g(F)$ defined in the text is shown in the inset of each figure. For all three cases, a linear behavior can be observed. In (b′) and (c′) the gaps A, B, C and D are presented by black circles, open black circles, open gray circles and open gray squares, respectively. The size of the system in all three cases corresponds to 1300 sites. In particular, in (a′) the relation can be considered as $\Delta E_g(F) = 1 - \alpha N F$, where $\alpha = 0.7666$.

where $k = 2n\pi/N$ and $n = 0, 1, \ldots, N-1$. To apply perturbation theory, we need to make two important remarks. The first is that each energy has double degeneration, corresponding to the eigenstates labeled by k and $-k$. The second is that, near the band edges, the degeneracy is increased since the distance between levels goes to zero, and thus leads to some problems that we will discuss later on. Having such problems in mind, we leave aside such problems for the moment. The energy correction is obtained by using degenerate perturbation theory [35]. This requires the eigenvalues of the reduced matrix H_F to be evaluated on the basis of the eigenstates $|k_n\rangle$ and $|-k_n\rangle$:

$$H_F = \begin{pmatrix} \langle k_n|H_F|k_n\rangle & \langle -k_n|H_F|k_n\rangle \\ \langle k_n|H_F|-k_n\rangle & \langle -k_n|H_F|-k_n\rangle \end{pmatrix}$$

where $|k_n\rangle = \exp(\mathrm{i}2\pi nj/N)/\sqrt{N}$ and $|k_n\rangle = \exp(-\mathrm{i}2\pi nj/N)/\sqrt{N}$. The energy correction for a periodic chain is

$$E^{(1)}_{\pm}(k) = \frac{F(N+1)}{2} \pm F\{\{N\cos[2k(N+1)] + (N+1)(2-N)\cos(2k) - (N+1)\cos(2Nk) - N\} \times \{2N^2(1-\cos(2ka))^2\}^{-1}\}^{1/2}. \quad (14)$$

If $N \gg 1$, the energy correction to $E^{(0)}(k)$ can be approximated by

$$E^{(1)}_{\pm}(k) \approx F\left(\frac{N}{2} \pm \frac{1}{\sqrt{2(1-\cos 2k)}}\right). \quad (15)$$

The previous formula shows that the effect of the field is to shift all energy levels by $FN/2$, while each degenerate level is split into two levels. Such an effect can be corroborated when we look at the energy corrections obtained directly from diagonalization. In figure 4(a), we plot the corrections obtained by diagonalization and using equation (15). One can see an excellent agreement at the center of the bands. However, at the band edges equation (15) predicts huge oscillations between the two solutions. In fact, when $k \to 0$, we have that

$$E^{(1)}_{\pm}(k) \approx F\left(\frac{N}{2} \pm \frac{1}{k}\right) = \frac{FN}{2}\left(1 \pm \frac{1}{\pi n}\right). \quad (16)$$

Such oscillations between the $+$ and $-$ solutions are not observed at the band edges. In spite of this, equation (15) seems to be a good approximation if the minus sign is chosen for $k \to 0$. For $n = 1$ this leads to the lowest energy level:

$$E \approx E^{(0)}_{\pm}(0) + \frac{FN}{2}\left(1 \pm \frac{1}{\pi}\right) \approx E^{(0)}_{\pm}(0) + \frac{FN}{3}. \quad (17)$$

A similar situation holds for $k \to \pi/2$, where the plus sign is a good approximation. In figure 4 we used this trick for the signs of equation (15), and it is clear that the results are good compared with the exact results from diagonalization.

The explanation for the sign rule is not so easy, for example, when $k \to 0$, and requires a careful examination of the behavior at the edges, since the level spacings go like $\mathrm{d}E^{(0)}(k)/\mathrm{d}k = 2t\sin(k) \approx 0$ and the states are almost degenerate. As a consequence, the matrix H_F will involve all eigenvectors n and m which satisfy $\langle n|H_F|m\rangle \gg E_n - E_m$. Although these matrix elements are easy to calculate, the size of the matrix does not allow us to visualize in a simple fashion the result. Thus, to gain insight about the problem, it is better to understand the nature of the solutions for $k \to 0$ and $k \to \pi/2$. In fact, the limiting cases of $k = 0$ and $\pi/2$ are easy to obtain using a variational procedure. For the lowest energy state $k = 0$, the effect of the field is to increase the self-energy as we move along the lattice. As a consequence, the ground state 'avoids' regions of high field to decrease its energy. At the same time, the ground state needs to have the minimum number of nodes and mix nearly degenerate eigenstates. This leads us to propose the following variational trial wavefunction for the ground state:

$$|\Psi\rangle = |k_0\rangle + \alpha(|k_1\rangle - |k_2\rangle). \quad (18)$$

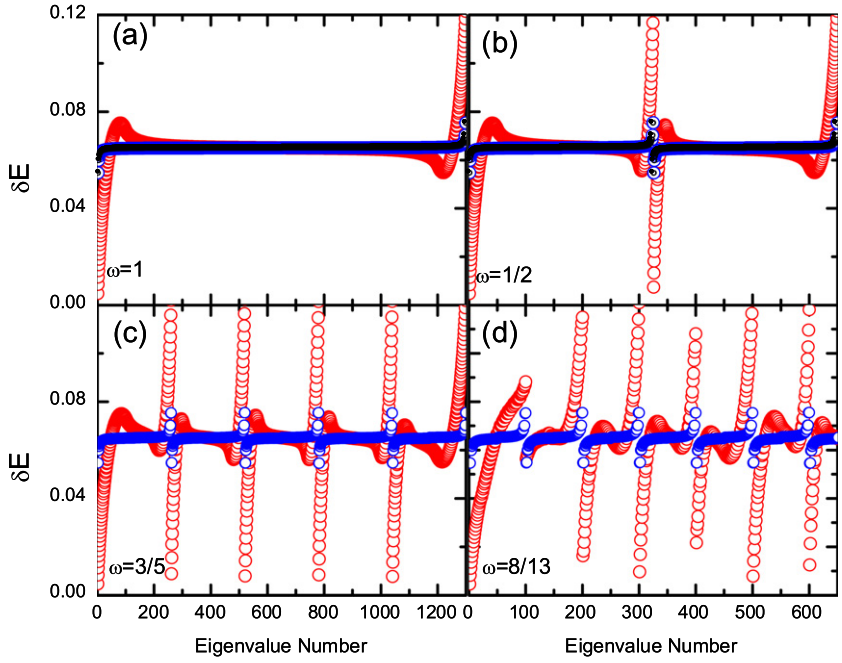

Figure 4. Energy correction (δE) versus the number of eigenvalues for a chain with 1300 sites and $F = 10^{-4}$ for four different Fibonacci approximants: (a) $\omega = 1$, (b) $\omega = 1/2$, (c) $\omega = 3/5$ and (d) $\omega = 8/13$. A good agreement is shown along all bands for each approximant between the diagonalization process (open light circles, red online) and perturbation theory (open dark circles, blue online). Equations (14) and (23) correspond to the analytic solution for the monatomic and the binary chains, respectively, and are shown with black circles in (a) and (b). The energy states in the band edges are the more drastically changed because H_F grows linearly with the size system. However, it can be obtained by a variational process (see the text).

In terms of the site representation

$$\psi(l) = \frac{1}{\sqrt{N}}\left[1 + \mu \sin\left(\frac{2\pi}{N} l\right)\right], \tag{19}$$

where μ is the variational parameter. The ground state energy is given by the minimal value of $\langle E\rangle = \langle\Psi|H|\Psi\rangle/\langle\Psi|\Psi\rangle$, which leads to

$$\langle E\rangle \simeq \frac{1}{1+\alpha^2}\left[E^{(0)}(0) + \frac{FN}{2} - \mu F \frac{\sin\left(\frac{2\pi}{N}\right)}{1-\cos\left(\frac{2\pi}{N}\right)} + \mu^2\left(E^{(0)}\left(\frac{2\pi}{N}\right) + \frac{FN}{4}\right)\right].$$

After a minimization procedure, we obtain

$$\langle E\rangle \simeq E^{(0)}(0) + \frac{FN}{3}. \tag{20}$$

Such a result is close to the observed numerical value obtained from diagonalization. Furthermore, it is equal to the value obtained from perturbation theory (see equation (17)) using the solution with the minus sign. The reason is the following. According to Anderson [36], under an electric field the wavefunctions must be as localized as possible to avoid regions of high field strength. As was shown by Blount [37], when wavefunctions are mixed due to the field, the phase of the wavefunctions become important. The mixing has the form [36]

$$|\Psi\rangle = \sum_n c(n)\, \mathrm{e}^{\mathrm{i}\phi_n}|k_n\rangle, \tag{21}$$

where $c(n)$ is an amplitude and ϕ_n a phase. This change of phase is very similar to a gauge transformation [37], and the phases are specified by the requirement that the $|\Psi\rangle$ must be as localized as possible [36]. Thus, the ground state which has the form $\psi(l) = \sin(2\pi l/N)$ is preferred, for example, to the linear combination that produces $\psi(l) = \cos(2\pi l/N)$, since the cosine has a maximum at the end of the chain where the field is also a maximum. A similar phenomena occurs for the highest eigenvalue but in the opposite direction, i.e. the phases are chosen to avoid regions of weak field. This explains why perturbation theory works provided that only one sign is chosen at the appropriate limit, because the phase is already fixed to minimize or maximize the energy.

Now let us consider the second approximant to the Fibonacci chain, which is given by $N/2$ atoms A and $N/2$ atoms B following the sequence $ABABABAB\cdots$ and periodic boundary conditions. If Bloch wavefunctions are proposed as solutions, the energy spectrum is

$$E_n = \tfrac{1}{2}(\epsilon_A + \epsilon_B) \pm \tfrac{1}{2}\sqrt{(\epsilon_A - \epsilon_B)^2 + 16t^2\cos^2(k)}, \tag{22}$$

where $k_n = 2\pi n/N$ and $n = 0, 1, \ldots, N/2$. The energy correction using degenerate perturbation theory can be written as

$$E_{\pm}^{(1)} = F\left[\frac{N}{2} + 1 - \frac{1}{1+\eta}\right] \pm C^2 F \sqrt{\frac{(1+\eta^2+2\eta\cos 2k)}{2(1-\cos 4k)^2}} \times \{2N(\cos[2k(N+2)] - 1) - (N+2)(N\cos 4k + 2\cos 2Nk - N - 2)\}^{1/2}, \tag{23}$$

where

$$\eta = \frac{4t^2\cos^2(k)}{(E-\epsilon_B)^2}, \tag{24}$$

and

$$C^2 = \frac{2}{N}\frac{1}{1+\eta}. \tag{25}$$

The energy gap in the binary chain appears at $k = \pi/2$ ($n = N/4$), with a gap width denoted by $\Delta E_g(F)$. Considering that $N \gg 1$ we can calculate $\Delta E_g(F)$ from equations (23) and (22):

$$\Delta E_g(F) = 1 - \frac{4F}{|\epsilon_A - \epsilon_B|}\sqrt{\frac{1}{2(1-\cos 4k)}}, \tag{26}$$

where we considered that $\eta = 0$ when $k \to \pi/2$. Using the identity $\cos 4k = \cos^2 2k - \sin^2 2k$ in the limit $k \to \pi/2$, and expanding in k using that $k = 2n\pi/N$, the equation is reduced to

$$\Delta E_g(F) \approx 1 - \frac{F}{|\epsilon_A - \epsilon_B|k} = 1 - \frac{FN}{2\pi|\epsilon_A - \epsilon_B|}. \tag{27}$$

The general expression for the gap can be written as

$$\Delta E_g(F) \approx 1 - \alpha N F, \tag{28}$$

where the α parameter is $1/(2\pi|\epsilon_A - \epsilon_B|)$. This proves that $\Delta E_g(F)$ goes linearly with the field F and N, as observed in the simulations shown in figure 3. A better approximation for α can be obtained by using a variational procedure as we made for the linear periodic chain.

The perturbation approach can be made for all other approximants. However, the basic mechanism for the spectral changes is already encoded in the study of the linear and diatomic chains. To understand this, first we define the energy correction $\delta E = E_F - E_0$, where E_F (E_0) is the energy with (without) the electric field. The numerical results were obtained using diagonalization and perturbation theory. In figure 4, δE is plotted versus the number of eigenvalues for a chain with 1300 sites and $F = 10^{-4}$ for four different Fibonacci approximants: (a) $\omega = 1$, (b) $\omega = 1/2$, (c) $\omega = 3/5$ and (d) $\omega = 8/13$. Notice that perturbation theory (open dark circles, blue online) is in good agreement with the diagonalization process (open light circles, red online) along all bands for each approximant. Equations (14) and (23) obtained from perturbation theory correspond to the monatomic and binary chain, respectively, and are shown by dark circles in figures 4(a) and (b). The process shown in figures 4(a)–(d) reveals how the energy correction is modified in the transition from the periodic to the quasiperiodic potentials. The energy states in the band edges are the more drastically changed because H_F grows linearly with the (size system) site number, as is easily seen in equation (14). Thus, in the quasiperiodic case, the evolution of each miniband is just a scaled version of what happens in the linear chain. Basically, the highest eigenvalue is raised, but at the same time, the lowest energy of each miniband is not changed in the same proportion. As a result, the gaps are closed. From a different perspective, such an idea is in agreement with an adiabatic approach applied to electric fields in periodic potentials. In that case, small energy gaps are easily jumped due to a high probability of tunneling [36].

5. Localization and participation ratio

In order to understand the effects of localization when a weak electric field is applied, we studied the participation ratio. This localization parameter is defined as

$$\mathrm{PR} \equiv \frac{1}{\sum_l |\psi_j(l)|^4}, \tag{29}$$

where $\psi_j(l)$ is the amplitude of eigenstate j at site l and the sum runs over all sites. Extended states have a PR that goes like N, while for localized states it has the order of the localization length. In the present work, we calculated the participation ratio by diagonalization of the same approximants considered in the previous section. In figure 5 we compare the PR for chains with zero electric field and a small field $F = 10^{-3}$. Figure 5(a) shows a monatomic chain ($\omega = 1$). The states tend to be more localized at the band edges when the electric field is applied. A similar behavior is observed for the binary chain ($\omega = 1/2$), as is depicted in figure 5(b), but in this case two bands are present. The same tendency is observed for the approximants $\omega = 3/5$ (figure 5(c)) and $\omega = 8/13$ (figure 5(d)). Following this sequence, it is possible to deduce that, for a Fibonacci chain, all the states tend to be more localized since many band edges appear.

Such an observation is in agreement with the fact that, in the limit of a strong field, all states are localized. However, due to the quantum tunneling effect, it is possible to have delocalization in some states when the electric field is increased. In fact, several delocalization effects have been reported in quasi-one-dimensional metals and for the Harper potential [23, 38, 39]. To look for such effects in the transition from the Harper to the Fibonacci potential, let us study one particular eigenstate as a function of the electric field. In this analysis, we choose a chain with 100 sites and the eigenstate 50, with $\omega = (\sqrt{5}-1)/2$, $t = 1$ and $\lambda = 1$. In figure 6(a), the Harper potential is shown and the first, fourth and hundredth Fibonacci harmonics are presented in figures 6(b)–(d), respectively. The general behavior is a tendency for localization when the electric field is increased, in good agreement with our previous results from sections 1 (see figure 1) and 2 (strong electric field). However, along the electric field axis there are some peaks indicating delocalization of the wavefunction. This behavior is easily corroborated by looking at the wavefunction. In the inset of figure 6(a), the wavefunction (Ψ_{50}) is shown for $F = 0.66$ (gray circles) in comparison with the same wavefunction with an electric field $F = 10$ (black circles). Notice how the strong localization is around site 50 for the second case ($F = 10$) and a light delocalization can be observed for the first one ($F = 0.66$). A similar behavior is observed for the Fibonacci harmonics where $F = 0.52$, 0.42 and 0.45, and for the first, fourth and hundredth harmonics, respectively.

The peaks are resonances in the chain. In order to understand such a process, let us analyze the Schrödinger equation:

$$[Fj + 2\lambda\cos(2\pi\omega j + \varphi)]\psi_n(j) + t[\psi_n(j-1) + \psi_n(j+1)] = E_n\psi_n(j).$$

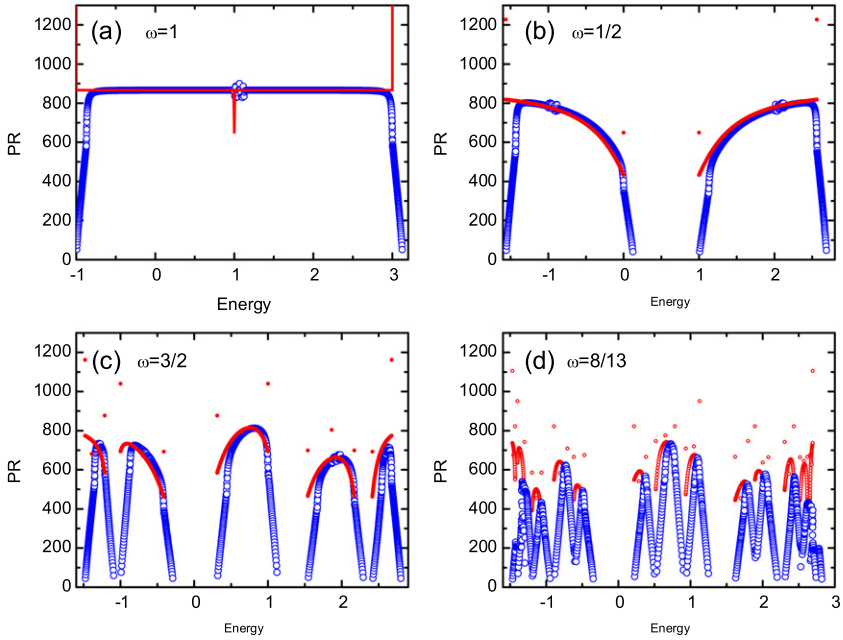

Figure 5. PR for different Fibonacci approximants using 1300 sites for zero field (dots) and $F = 10^{-3}$ (open circles). (a) $\omega = 1$ corresponding to a monatomic chain. The field tends to localize states at the band edge of the band. A similar phenomena is observed for (b) $\omega = 1/2$, (c) $\omega = 3/5$ and (d) $\omega = 8/13$.

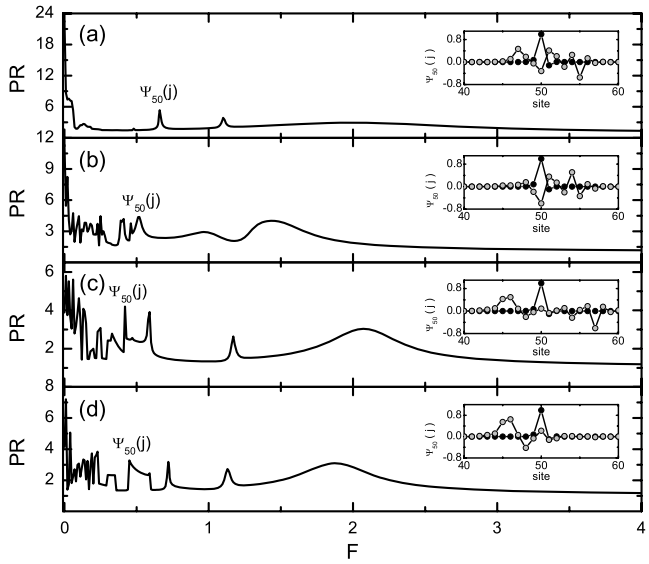

Figure 6. Participation ratio (PR) as a function of the electric field (F) for the eigenfunction number 50 (Ψ_{50}) in a chain with 100 sites. (a) Harper potential, (b) second, (c) fourth and (d) hundredth Fibonacci harmonics, respectively. Along the electric field axis, one can observe some resonances where the wavefunction is delocalized. In the inset of each figure, the wavefunction around site 50 is presented (gray circles) for different electrical fields: (a) $F = 0.66$, (b) $F = 0.52$, (c) $F = 0.42$ and (d) $F = 0.45$, in comparison with the same wave with a strong electric field $F = 10$ (black circles). Notice the strong localization around site 50 for the $F = 10$ case, while a slight delocalization can be observed at the other fields.

Localized states appear as a consequence of the term $Fj + 2\lambda\cos(2\pi\omega j + \varphi)$, while extended states are driven by the kinetic term proportional to t. In the limit when the on-site potential has the same order of magnitude of the electric field, i.e. $Fj \approx 2\lambda$, locally it is possible to reduce the localization effect when $\cos(2\pi\omega j + \varphi) \approx -1$, since $Fj - 2\lambda \approx 0$. This analysis is corroborated in the inset of figure 6, since for eigenvalue 50, a slight delocalization is observed. It is worth mentioning that, although a delocalization effect can be appreciated for different electric fields, this delocalization is not enough to imply an important effect over the system.

6. Conclusions

In this paper, we explored the effects of an electric field on the electronic spectrum of quasiperiodic potentials. Our results indicate that, in the limit of a strong field, the spectrum is a ladder with a structure that has the shape of the quasiperiodic potential. In the limit of weak fields, the states tend to be localized in order to avoid regions of strong or weak fields, and a smoothening effect of the original spectrum is observed.

Acknowledgments

We thank DGAPA-UNAM projects IN100310-3, IN-111906 and CONACyT 48783-F and 50368. FS thanks CONACYT and Posgrado de Ciencias Físicas, UNAM for a postdoctoral scholarship. The calculations were performed at the Kanbalam and Bakliz supercomputers at DGSCA-UNAM.

References

[1] Shechtman D, Blech I, Gratias D and Cahn J W 1984 *Phys. Rev. Lett.* **53** 1951
[2] Kohmoto M and Sutherland B 1987 *Phys. Rev.* B **35** 1020
[3] Ostlund S *et al* 1983 *Phys. Rev.* B **50** 1873
[4] Kohmoto M and Banavar J R 1986 *Phys. Rev.* B **34** 563

[5] Hiramoto H and Kohmoto M 1989 *Phys. Rev.* B **40** 8225
[6] López J C, Naumis G and Aragón J L 1993 *Phys. Rev.* B **48** 12459
[7] Naumis G G 1999 *Phys. Rev.* B **59** 11315
[8] Aubry S and Andre G 1979 *Colloquium on Group Theoretical Methods in Physics* ed K Anavim (New York: American Institute of Physics)
Reprinted in: Steinhard P and Ostlund S 1987 *The Physics of Quasicrystals* (Singapore: World Scientific)
[9] Naumis G G 2004 *Ferroelectrics* **305** 137
[10] Thiel P A and Dubois J M 2000 *Nature* **406** 570
[11] Maciá E and Domínguez-Adame F 1997 *Phys. Rev. Lett.* **79** 5301
[12] Sánchez V *et al* 2001 *Phys. Rev.* B **64** 174205
[13] Naumis G G and Aragón J L 1996 *Phys. Rev.* B **54** 15079
[14] Naumis G G and Aragón J L 1998 *Phys. Lett.* A **244** 133
[15] Naumis G G, Wang Ch, Thorpe M F and Barrio R A 1999 *Phys. Rev.* B **59** 14302
[16] Naumis G G 2003 *J. Phys.: Condens. Matter* **15** 5969
[17] Naumis G G 2005 *Phys. Rev.* B **71** 144204
[18] Naumis G G 2006 *Phys. Rev.* B **73** 172202
[19] Sánchez V and Wang C 2004 *Phys. Rev.* B **70** 144207
[20] Macia E 2006 *Rep. Prog. Phys.* **69** 397
[21] Wang C, Salazar F and Sánchez V 2008 *Nano Lett.* **8** 4205
[22] Weisz J F and Slutzky C 1986 *Phys. Rev.* B **34** 4162
[23] Weisz J F 1988 *Phys. Rev.* B **37** 4781
[24] Nazareno H N, de Brito P E and da Silva C A A 1995 *Phys. Rev.* B **51** 864
[25] Luban M and Luscombe J H 1986 *Phys. Rev.* B **34** 3674
[26] Wannier G H 1960 *Phys. Rev.* **117** 432
[27] Wannier G H 1962 *Rev. Mod. Phys.* **34** 645
[28] Niizeki K and Matsumura A 1993 *Phys. Rev.* B **48** 4126
[29] Carpena P, Gasparian V and Ortuño M 1997 *Z. Phys.* B **102** 425
[30] Naumis G G and López-Rodríguez F J 2008 *Physique* B **403** 1755
[31] Voising P *et al* 1988 *Phys. Rev. Lett.* **61** 1639
[32] Schneider H, Grahn H T, von Klitzing V and Ploog K 1990 *Phys. Rev. Lett.* **65** 2720
[33] Sapienza R, Constantino P and Wiersma D 2003 *Phys. Rev. Lett.* **91** 263902
[34] Hofstadter D R 1976 *Phys. Rev.* B **14** 2239
[35] Griffiths D J 2005 *Introduction to Quantum Mechanics* 2nd edn (Englewood Cliffs, NJ: Pearson Prentice-Hall) p 257
[36] Anderson P W 1997 *Concepts in Solids* (Singapore: World Scientific)
[37] Blount E I 1962 *Phys. Rev.* **126** 1636
[38] Barden J 1985 *Phys. Rev. Lett.* **55** 1010
[39] Thorne R E *et al* 1985 *Phys. Rev. Lett.* **55** 1006